Differential global distribution of marine picocyanobacteria gene clusters reveals distinct niche-related adaptive strategies

Hugo Doré, Ulysse Guyet, Jade Leconte, Gregory Farrant, Benjamin Alric, Morgane Ratin, Martin Ostrowski, Mathilde Ferrieux, Loraine Brillet-Guéguen, Mark Hoebeke, et al.

Differential global distribution of marine picocyanobacteria gene clusters reveals distinct niche-related adaptive strategies

Hugo Doré[a,1], Ulysse Guyet[a,1], Jade Leconte[a], Gregory K. Farrant[a], Benjamin Alric[a], Morgane Ratin[a], Martin Ostrowski[b,2], Mathilde Ferrieux[a], Loraine Brillet-Guéguen[c,d], Mark Hoebeke[c], Jukka Siltanen[c], Gildas Le Corguillé[c], Erwan Corre[c], Patrick Wincker[f,g], David J. Scanlan[b], Damien Eveillard[h,g], Frédéric Partensky[a], and Laurence Garczarek[a,g,*]

[a]Sorbonne Université, CNRS, UMR 7144 Adaptation and Diversity in the Marine Environment (AD2M), Station Biologique de Roscoff (SBR), Roscoff, France; [b]School of Life Sciences, University of Warwick, Coventry CV4 7AL, UK; [c]CNRS, FR 2424, ABiMS Platform, Station Biologique de Roscoff (SBR), Roscoff, France; [d]Sorbonne Université, CNRS, UMR 8227, Integrative Biology of Marine Models (LBI2M), Station Biologique de Roscoff (SBR), Roscoff, France; [e]Genoscope, Institut de biologie François-Jacob, Commissariat à l'Energie Atomique (CEA), Université Paris-Saclay, Evry, France; [f]Génomique Métabolique, Genoscope, Institut de biologie François Jacob, CEA, CNRS, Université d'Evry, Université Paris-Saclay, Evry, France; [g]Research Federation (FR2022) *Tara* Océans GO-SEE, Paris, France; [h]Nantes Université, Centrale Nantes, CNRS, LS2N, UMR 6004, Nantes, France.

[1]H.D. and U.G. contributed equally to this work

[2]Current address: Climate Change Cluster, University of Technology, Broadway NSW 2007, Australia

[*]To whom correspondence should be addressed. Email: laurence.garczarek@sb-roscoff.fr. phone number: +33 2 98 29 25 38

Running Title: Niche adaptation strategies in marine picocyanobacteria

Competing Interest Statement: The authors declare no competing interests.

Keywords: *Prochlorococcus, Synechococcus,* niche partitioning, *Tara* Oceans, metagenomics

Abstract

The ever-increasing number of available microbial genomes and metagenomes provides new opportunities to investigate the links between niche partitioning and genome evolution in the ocean, especially for the abundant and ubiquitous marine picocyanobacteria *Prochlorococcus* and *Synechococcus*. Here, by combining metagenome analyses of the *Tara* Oceans dataset with comparative genomics, including phyletic patterns and genomic context of individual genes from 256 reference genomes, we show that picocyanobacterial communities thriving in different niches possess distinct gene repertoires. We also identify clusters of adjacent genes that display specific distribution patterns in the field (eCAGs) and are thus potentially involved in the same metabolic pathway and may have a key role in niche adaptation. Several eCAGs are likely involved in the uptake or incorporation of complex organic forms of nutrients, such as guanidine, cyanate, cyanide, pyrimidine, or phosphonates, which might be either directly used by cells, for example the biosynthesis of proteins or DNA, or degraded to inorganic nitrogen and/or phosphorus forms. We also highlight the enrichment of eCAGs involved in polysaccharide capsule biosynthesis in *Synechococcus* populations thriving in both nitrogen- and phosphorus-depleted areas vs. low-iron (Fe) regions, suggesting that the complexes they encode may be too energy-consuming for picocyanobacteria thriving in the latter areas. In contrast, *Prochlorococcus* populations thriving in Fe-depleted areas specifically possess an alternative respiratory terminal oxidase, potentially involved in the reduction of Fe(III) to Fe(II). Altogether, this study provides insights into how phytoplankton communities populate oceanic ecosystems, which is relevant to understanding their capacity to respond to ongoing climate change.

Introduction

Although phytoplankton communities play a crucial role in marine biogeochemical cycles [1, 2], the relative contribution of different species or ecotypes to these cycles remains difficult to assess due to a lack of knowledge of specific metabolic traits. Indeed, trait-based functional diversity is thought to be a better predictor of ecosystem functioning than species diversity [3, 4], and understanding which metabolic traits have facilitated the adaptation of an ecotype to a particular environment is key to understanding each species' ecological role. Comparative genomics has sometimes been used to try to identify the genetic basis of niche adaptation. However, this

approach has revealed only a few genes specific to particular ecotypes and thus potentially involved in niche adaptation, perhaps due to the fairly low number of genomes available (even for major phytoplankton groups) and the poor ecological representation and physiological characterization of available isolates [5–9]. An alternative to better deciphering the links between functional diversity and niche partitioning involves exploiting the rapidly growing number of metagenomes. These can be used to generate metagenome-assembled genomes (MAGs) that can fill the gaps for yet uncultured microbial taxa as well as to identify niche-specific genes, i.e. genes enriched in specific spatial and/or temporal environmental conditions, by recruiting metagenomic reads onto reference genomes [10–16].

Due to their abundance and ubiquity in the field and the large number of available genomes, including single amplified genomes (SAGs) and MAGs [6, 17–20], the marine picocyanobacteria *Prochlorococcus* and *Synechococcus* constitute highly pertinent models to study how phytoplankton cells adapt to their variable physico-chemical environment. These genera are indeed the two most abundant members of the phytoplankton community, *Prochlorococcus* being restricted to the 40°S-50°N latitudinal band, whilst the distribution of *Synechococcus* extends from the equator to subpolar waters [21–23]. By combining laboratory and environmental studies scientists have managed to decipher their genetic diversity and delineate specific ecotypes or "ecologically significant taxonomic units" (ESTUs), i.e. genetic groups within clades occupying a specific ecological niche [24–28]. While three major ESTU assemblages were identified for *Prochlorococcus* in surface waters, whose distribution was found to be mainly driven by temperature and iron (Fe) availability, eight distinct assemblages were identified for *Synechococcus* depending on three main environmental parameters: temperature, Fe, and phosphorus (P) availability. Nevertheless, few studies have so far linked knowledge of the distribution of the different ecotypes to their functional diversity in order to identify potential niche-specific genes, based on gene relative abundance in different ecosystems [10, 14, 15, 29, 30]. Furthermore, most of these previous studies have focused on the abundance of individual genes, or more rarely, on just a few genomic regions with known function, for example those involved in nitrogen (N) or P uptake and assimilation [31–33].

Here, in order to better understand the relationship between biogeochemistry and metabolic traits of marine picocyanobacteria, we searched for global patterns of picocyanobacterial gene

distributions. To do so, we used a network approach to integrate metagenome analyses of the oceanwide *Tara* Oceans dataset and synteny of individual accessory genes in 256 reference genomes, SAGs, or MAGs covering the wide diversity existing within *Prochlorococcus* and *Synechococcus.* Using this approach, we identified many clusters of adjacent genes that display distinctive global distribution patterns *in situ* and thus likely play important roles in the adaptation of these bacteria to the main ecological niches they occupy in the ocean. Given that gene synteny is commonly used as an indicator of shared function [34, 35], delineation of these gene clusters should also help to identify the putative function of numerous unknown genes, based on their occurrence alongside functionally annotated genes in the same cluster. Overall, this study provides novel insights into the genetic basis of niche partitioning in key members of the phytoplankton community.

Results and Discussion

Different picocyanobacterial communities exhibit distinct gene repertoires

To analyze the distribution of *Prochlorococcus* and *Synechococcus* reads along the *Tara* Oceans transect, metagenomic reads corresponding to the bacterial size fraction were recruited against 256 picocyanobacterial reference genomes, including SAGs and MAGs representative of uncultured lineages (e.g. *Prochlorococcus* HLIII-IV, *Synechococcus* EnvA or EnvB). This yielded a total of 1.07 billion recruited reads, of which 87.7% mapped onto *Prochlorococcus* genomes and 12.3% onto *Synechococcus* genomes, which were then functionally assigned by mapping them onto the manually curated Cyanorak *v2.1* CLOG database [19]. In order to identify picocyanobacterial genes potentially involved in niche adaptation, we analyzed the distribution across the oceans of flexible (i.e. non-core) genes. Clustering of *Tara* Oceans stations according to the relative abundance of flexible genes resulted in three well-defined clusters for *Prochlorococcus* (Fig. 1A), which matched those obtained when stations were clustered according to the relative abundance of *Prochlorococcus* ESTUs, as assessed using the high-resolution marker gene *petB,* encoding cytochrome b_6 (Fig. 1A; [24]). Only a few discrepancies can be observed between the two trees, including stations TARA-070 that displayed one of the most disparate ESTU compositions and TARA-094, dominated by the rare HLID ESTU (Fig. 1A). Similarly, for *Synechococcus*, most of the eight assemblages of stations discriminated based on the relative

abundance of ESTUs (Fig. 1B) were also retrieved in the clustering based on flexible gene abundance, except for a few intra-assemblage switches between stations, notably those dominated by ESTU IIA (Fig. 1B). Despite these few variations, four major clusters can be clearly delineated in both *Synechococcus* trees, corresponding to four broadly defined ecological niches, namely i) cold, nutrient-rich, pelagic or coastal environments (blue and light red in Fig. 1B), ii) Fe-limited environments (purple and grey), iii) temperate, P-depleted, Fe-replete areas (yellow) and iv) warm, N-depleted, Fe-replete regions (dark red). This correspondence between taxonomic and functional information was also confirmed by the high congruence between distance matrices based on ESTU relative abundance and on CLOG relative abundance (p value<10^{-4}, mantel test r=0.84 and r=0.75 for *Synechococcus* and *Prochlorococcus,* respectively; dataset 1-4). Altogether, this indicates that distinct picocyanobacterial communities, as assessed based on a single taxonomic marker, also display different gene repertoires. As previously suggested for *Prochlorococcus* [36], this strong correlation between taxonomy and gene content strengthens the idea that, in both genera, the evolution of the accessory genome mainly occurs by vertical transmission, with a relatively low extent of lateral gene transfers, although we cannot exclude that the latter events may occur more often within members of a given ecotype.

Distribution of flexible genes is tightly linked to environmental parameters and ESTUs

In order to reduce the amount of data and better interpret the global distribution of picocyanobacterial gene content, a correlation network of genes was built for each genus based on relative abundance profiles of genes across *Tara* Oceans samples using Weighted Correlation Network Analysis (WGCNA). This analysis emphasized four main modules of genes for *Prochlorococcus* (Fig. S1A) and five for *Synechococcus* (Fig. S1B), each module being abundant in a different set of stations. These modules were then associated with the available environmental parameters (Figs. 2A-B) and to the relative abundance of *Prochlorococcus* or *Synechococcus* ESTUs at each station (Figs. 2C-D). For instance, the *Prochlorococcus brown* module was strongly correlated with nutrient concentrations, particularly nitrate and phosphate, and strongly anti-correlated with Fe availability (Fig. 2A). This module thus corresponds to genes preferentially found in Fe-limited high-nutrient low-chlorophyll (HNLC) areas. Indeed, the *brown* module *eigengene* (Fig. S1A), i.e. the first principal component of gene abundances at the different stations for this module, representative of the abundance profiles of genes for this module at the

different stations, showed the highest abundances at stations TARA-100 to 125, localized in the South and North Pacific Ocean, as well as at TARA-052, a station located close to the northern coast of Madagascar, likely influenced by the Indonesian throughflow originating from the tropical Pacific Ocean [24, 37]. Furthermore, the correlation of the *Prochlorococcus brown* module with the relative abundance of ESTUs at each station showed that it is also strongly associated with the presence of HLIIIA and HLIVA (Fig. 2C), previously shown to constitute the dominant *Prochlorococcus* ESTUs in low-Fe environments [24, 38, 39] but also the LLIB ESTU, found to dominate the LLI population in these low-Fe areas [24]. Altogether, this example and analyses of all other *Prochlorococcus* and *Synechococcus* modules (supplementary text) show that the communities colonizing cold, Fe-, N-, and/or P-depleted niches possess specific gene repertoires potentially involved in their adaptation to these particular environmental conditions.

Identification of individual genes potentially involved in niche partitioning

To identify genes relevant for adaptation to a specific set of environmental conditions and enriched in specific ESTU assemblages, we selected the most representative genes from each module (Dataset 5, Figs. 3 and S2). Most genes retrieved this way encode proteins of unknown or hypothetical function (85.7% of 7,485 genes). However, among the genes with a functional annotation (Dataset 6), a large fraction seems to have a function related to their realized environmental niche (Figs. 3 and S2). For instance, many genes involved in the transport and assimilation of nitrite and nitrate (*nirA*, *nirX*, *moaA-C, moaE, mobA, moeA, narB, M, nrtP;* [6]) as well as cyanate, an organic form of nitrogen (*cynA, B, D, S*), are enriched in the *Prochlorococcus blue* module, which is correlated with the HLIIA-D ESTU and to low inorganic N, P, and silica levels and anti-correlated with Fe availability (Fig. 2A-C). This is consistent with previous studies showing that while only a few *Prochlorococcus* strains in culture possess the *nirA* gene and even less the *narB* gene, natural *Prochlorococcus* populations inhabiting N-poor areas do possess one or both of these genes [40–42]. Similarly, numerous genes amongst the most representative of *Prochlorococcus brown, red* and *turquoise* modules are related to adaptation of HLIIIA/IVA, HLIA and LLIA ESTUs to Fe-limited, cold P-limited, and cold, mixed waters, respectively (Fig. 3). Comparable results were obtained for *Synechococcus,* although the niche delineation was less clear than for *Prochlorococcus* since genes within each module exhibited lower correlations with

the module *eigenvalue* (Fig. S2). These results therefore constitute a proof of concept that this network analysis was able to retrieve niche-related genes from metagenomics data.

Identification of eCAGs potentially involved in niche partitioning

In order to better understand the function of niche-related genes, notably of the numerous unknowns, we then integrated global distribution data with gene synteny in reference genomes using a network approach (Datasets 7 and 8). This led us to identify clusters of adjacent genes in reference genomes, and thus potentially involved in the same metabolic pathway (Figs. 4, S3 and S4; Dataset 6). These clusters were defined within each module and thus encompass genes with similar distribution and abundance *in situ*. Hereafter, these environmental clusters of adjacent genes will be called "eCAGs".

eCAGs related to nitrogen metabolism

The well-known nitrate/nitrite gene cluster involved in uptake and assimilation of inorganic forms of N (see above), which is present in most *Synechococcus* genomes (Dataset 6), was expectedly not restricted to a particular niche in natural *Synechococcus* populations, as shown by its quasi-absence from WGCNA modules. In *Prochlorococcus*, this cluster is separated into two eCAGs enriched in low-N areas (Fig. S5A-B), most genes being included in Pro-eCAG_002, present in only 13 out of 118 *Prochlorococcus* genomes, while *nirA* and *nirX* form an independent eCAG (Pro-eCAG_001) due to their presence in many more genomes. The quasi-core *ureA-G*/*urtB-E* genomic region was also found to form a *Prochlorococcus* eCAG (Pro-eCAG_003) that was impoverished in low-Fe compared to other regions (Fig. S5C-D), in agreement with its presence in only two out of six HLIII/IV genomes. We also uncovered several other *Prochlorococcus* and *Synechococcus* eCAGs that seem to be involved in the transport and/or assimilation of more unusual and/or complex forms of nitrogen, which might either be degraded into elementary N molecules or possibly directly used by cells for e.g. the biosynthesis of proteins or DNA. Indeed, we detected in both genera an eCAG (Pro-eCAG_004 and Syn-eCAG_001 ; Figs. S6A-B, Dataset 6) that encompasses *speB2*, an ortholog of *Synechocystis* PCC 6803 *sll1077*, previously annotated as encoding an agmatinase [29, 43] and which was recently characterized as a guanidinase that degrades guanidine rather than agmatine to urea and ammonium [44]. *E. coli* produces guanidine

under nutrient-poor conditions, suggesting that guanidine metabolism is biologically significant and potentially prevalent in natural environments [44, 45]. Furthermore, the *ykkC* riboswitch candidate, which was shown to specifically sense guanidine and to control the expression of a variety of genes involved in either guanidine metabolism or nitrate, sulfate, or bicarbonate transport, is located immediately upstream of this eCAG in *Synechococcus* reference genomes, all genes of this cluster being predicted by RegPrecise 3.0 to be regulated by this riboswitch (Fig. S6C; [45, 46]). The presence of *hypA* and *B* homologs within this eCAG furthermore suggests that, in the presence of guanidine, these homologs could be involved in the insertion of Ni_2^+, or another metal cofactor, in the active site of guanidinase. The next three genes of this eCAG, which encode an ABC transporter similar to the TauABC taurine transporter in *E. coli* (Fig. S6C), could be involved in guanidine transport in low-N areas. Of note, the presence in most *Synechococcus*/*Cyanobium* genomes possessing this eCAG of a gene encoding a putative Rieske Fe-sulfur protein (CK_00002251) downstream of this gene cluster, seems to constitute a specificity compared to the homologous gene cluster in *Synechocystis* sp. PCC 6803. The presence of this Fe-S protein suggests that Fe is used as a cofactor in this system and might explain why this gene cluster is absent from picocyanobacteria thriving in low-Fe areas, while it is present in a large proportion of the population in most other oceanic areas (Figs. S6A-B).

Another example of the use of organic N forms concerns compounds containing a cyano radical (C≡N). The cyanate transporter genes (*cynABD*) were indeed found in a *Prochlorococcus* eCAG (Pro-eCAG_005, also including the conserved hypothetical gene CK_00055128; Fig. S7A-B). While only a small proportion of the *Prochlorococcus* community possesses this eCAG in warm, Fe-replete waters, it is absent from other oceanic areas in accordance with its low frequency in *Prochlorococcus* genomes (present in only two HLI and five HLII genomes). In *Synechococcus* these genes were not included in a module, and thus are not in an eCAG (Dataset 6; Fig. S7C), but seem widely distributed despite their presence in only a few *Synechococcus* genomes (mostly in clade III strains; [6, 47, 48]). Interestingly, we also uncovered a 7-gene eCAG (Pro-eCAG_006 and Syn-eCAG_002), encompassing a putative nitrilase gene (*nitC*), which also suggests that most *Synechococcus* cells and a more variable fraction of the *Prochlorococcus* population could use nitriles or cyanides in warm, Fe-replete waters and more particularly in low-N areas such as the Indian Ocean (Fig. 5A-B). The whole operon (*nitHBCDEFG;* Fig. 5C), called Nit1C, was shown to be

upregulated in the presence of cyanide and to trigger an increase in the rate of ammonia accumulation in the heterotrophic bacterium *Pseudomonas fluorescens* [49], suggesting that like cyanate, cyanide could constitute an alternative nitrogen source in marine picocyanobacteria as well. However, given the potential toxicity of these C≡N-containing compounds [50], we cannot exclude that these eCAGs could also be devoted to cell detoxification [45, 47]. Such an example of detoxification has been described for arsenate and chromate that, as analogs of phosphate and sulfate respectively, are toxic to marine phytoplankton and must be actively exported out of the cells [51, 52].

We detected the presence of an eCAG encompassing *asnB, pyrB2,* and *pydC* (Pro-eCAG_007, Syn-eCAG_003, Fig. S8), which could contribute to an alternative pyrimidine biosynthesis pathway and thus provide another way for cells to recycle complex nitrogen forms. While this eCAG is found in only one fifth of HLII genomes and in quite specific locations for *Prochlorococcus*, notably in the Red Sea, it is found in most *Synechococcus* cells in warm, Fe-replete, N and P-depleted niches, consistent with its phyletic pattern showing its absence only from most clade I, IV, CRD1, and EnvB genomes (Fig. S8; Dataset 6). More generally, most N-uptake and assimilation genes in both genera were specifically absent from Fe-depleted areas, including the *nirA/narB* eCAG for *Prochlorococcus,* as mentioned by Kent et al. [36] as well as guanidinase and nitrilase eCAGs. In contrast, picocyanobacterial populations present in low-Fe areas possess, in addition to the core ammonium transporter *amt1,* a second transporter *amt2*, also present in cold areas for *Synechococcus* (Fig. S9). Additionally, *Prochlorococcus* populations thriving in HNLC areas also possess two amino acid-related eCAGs that are present in most *Synechococcus* genomes, the first one involved in polar amino acid N-II transport (Pro-eCAG_008; *natF-G-H-bgtA;* [53]; Fig. S10A-B) and the second one (*leuDH-soxA*-CK_00001744, Pro-eCAG_009, Fig. S10C-D) that notably encompasses a leucine dehydrogenase, able to produce ammonium from branched-chain amino acids. This highlights the profound difference in N acquisition mechanisms between HNLC regions and Fe-replete, N-deprived areas: the primary nitrogen sources for picocyanobacterial populations dwelling in HNLC areas seem to be ammonium and amino acids, while N acquisition mechanisms are more diverse in N-limited, Fe-replete regions.

eCAGs related to phosphorus metabolism

Adaptation to P depletion has been well documented in marine picocyanobacteria showing that while in P-replete waters *Prochlorococcus* and *Synechococcus* essentially rely on inorganic phosphate acquired by core transporters (PstSABC), strains isolated from low-P regions and natural populations thriving in these areas additionally contain a number of accessory genes related to P metabolism, located in specific genomic islands [6, 14, 30–32, 54]. Here, we indeed found in *Prochlorococcus* an eCAG containing the *phoBR* operon (Pro-eCAG_010) that encodes a two-component system response regulator, as well as an eCAG including the alkaline phosphatase *phoA* (Pro-eCAG_011), both present in virtually the whole *Prochlorococcus* population from the Mediterranean Sea, the Gulf of Mexico and the Western North Atlantic Ocean, which are known to be P-limited [30, 55] (Fig. S11A-B). By comparison, in *Synechococcus,* we only identified the *phoBR* eCAG (Syn-eCAG_005, Fig. S11C) that is systematically present in warm waters whatever the limiting nutrient, in agreement with its phyletic pattern in reference genomes showing its specific absence from cold thermotypes (clades I and IV, Dataset 6). Furthermore, although our analysis did not retrieve them within eCAGs due to the variability of gene content and synteny in this genomic region, even within each genus, several other P-related genes were enriched in low-P areas but partially differed between *Prochlorococcus* and *Synechococcus* (Figs. 3, S2, S11 and Dataset 6). While the genes putatively encoding a chromate transporter (ChrA) and an arsenate efflux pump ArsB were present in both genera in different proportions, a putative transcriptional phosphate regulator related to PtrA (CK_00056804; [56]) was specific to *Prochlorococcus*. *Synechococcus* in contrast harbors a large variety of alkaline phosphatases (PhoX, CK_00005263 and CK_00040198) as well as the phosphate transporter SphX (Fig. S11).

Phosphonates, i.e. reduced organophosphorus compounds containing C–P bonds that represent up to 25% of the high-molecular-weight dissolved organic P pool in the open ocean, constitute an alternative P form for marine picocyanobacteria [57]. We indeed identified, in addition to the core phosphonate ABC transporter (*phnD1-C1-E1*), a second previously unreported putative phosphonate transporter *phnC2-D2-E2-E3* (Pro-eCAG_012; Fig. 6A). Most of the *Prochlorococcus* population in strongly P-limited areas of the ocean harbored these genes, while they were absent from other areas, consistent with their presence in only a few *Prochlorococcus* and no *Synechococcus* genomes. Furthermore, as previously described [58–60],

we found a *Prochlorococcus* eCAG encompassing the *phnYZ* operon involved in C-P bond cleavage, the putative phosphite dehydrogenase *ptxD*, and the phosphite and methylphosphonate transporter *ptxABC* (Pro-eCAG_0013, Dataset 6, and Fig. 6B, [60–62]). Compared to these previous studies that mainly reported the presence of these genes in *Prochlorococcus* cells from the North Atlantic Ocean, here we show that they actually occur in a much larger geographic area, including the Mediterranean Sea, the Gulf of Mexico, and the ALOHA station (TARA_132) in the North Pacific, even though they were present in a fairly low fraction of *Prochlorococcus* cells. These genes occurred in an even larger proportion of the *Synechococcus* population, although not found in an eCAG for this genus (Fig. S12, Dataset 6). *Synechococcus* cells from the Mediterranean Sea, a P-limited area dominated by clade III [24], seem to lack *phnYZ,* in agreement with the phyletic pattern of these genes in reference genomes, showing the absence of this two-gene operon in the sole clade III strain that possesses the *ptxABDC* gene cluster. In contrast, the presence of the complete gene set (*ptxABDC-phnYZ*) in the North Atlantic, at the entrance of the Mediterranean Sea, and in several clade II reference genomes rather suggests that it is primarily attributable to this clade. Altogether, our data indicate that part of the natural populations of both *Prochlorococcus* and *Synechococcus* would be able to assimilate phosphonate and phosphite as alternative P-sources in low-P areas using the *ptxABDC-phnYZ* operon. Yet, the fact that no picocyanobacterial genome except *P. marinus* RS01 (Fig. 6C) possesses both *phnC2-D2-E2-E3* and *phnYZ,* suggests that the phosphonate taken up by the *phnC2-D2-E2-E3* transporter could be incorporated into cell surface phosphonoglycoproteins that may act to mitigate cell mortality by grazing and viral lysis, as recently suggested [63].

eCAGs related to iron metabolism

As for macronutrients, it has been hypothesized that the survival of marine picocyanobacteria in low-Fe regions was made possible through several strategies, including the loss of genes encoding proteins that contain Fe as a cofactor, the replacement of Fe by another metal cofactor, and the acquisition of genes involved in Fe uptake and storage [14, 15, 36, 39, 64]. Accordingly, several eCAGs encompassing genes encoding proteins interacting with Fe were found in modules anti-correlated to HNLC regions in both genera. These include three subunits of the (photo)respiratory complex succinate dehydrogenase (SdhABC*,* Pro-eCAG_014, Syn-eCAG_006, Fig. S13; [65]) and

Fe-containing proteins encoded in most abovementioned eCAGs involved in N or P metabolism, such as the guanidinase (Fig. S6), the NitC1 (Fig. 5), the *pyrB2* (Fig. S8), the phosphonate (Figs. 6 and S12), and the urea and inorganic nitrogen eCAGs (Fig. S5). Most *Synechococcus* cells thriving in Fe-replete areas also possess the *sodT*/*sodX* eCAG (Syn-eCAG_007, Fig. S14A-B) involved in nickel transport and maturation of the Ni-superoxide dismutase (SodN), these three genes being in contrast core in *Prochlorococcus.* Additionally, *Synechococcus* from Fe-replete areas, notably from the Mediterranean Sea and the Indian Ocean, specifically possess two eCAGs (Syn-eCAG_008 and 009; Fig. S14C-D), involved in the biosynthesis of a polysaccharide capsule that appear to be most similar to the *E. coli* groups 2 and 3 *kps* loci [66]. These extracellular structures, known to provide protection against biotic or abiotic stress, were recently shown in *Klebsiella* to provide a clear fitness advantage in nutrient-poor conditions since they were associated with increased growth rates and population yields [67]. However, while these authors suggested that capsules may play a role in Fe uptake, the significant reduction in the relative abundance of *kps* genes in low-Fe compared to Fe-replete areas (t-test p value <0.05 for all genes of the Syn-eCAG_008 and 009; Fig. S14C) and their absence in CRD1 strains (Dataset 6) rather suggests that these capsules may be too energy-consuming for some picocyanobacteria thriving in this particular niche, while they may have a more meaningful and previously overlooked role in their adaptation to low-P and low-N niches.

Several eCAGs were in contrast enriched in populations dwelling in HNLC environments, dominated by *Prochlorococcus* HLIIIA/HLIVA/LLIB and *Synechococcus* CRD1A/EnvBA ESTUs (Fig. 2). The vast majority of *Prochlorococcus* cells thriving in low-Fe regions possess an eCAG encompassing the *ctaC2-D2-E2* operon, also found in 85% of all *Synechococcus* reference genomes, including all CRD1 (Fig. 7; Dataset 6). This eCAG encodes the alternative respiratory terminal oxidase ARTO, a protein complex that has been suggested to be part of a minimal respiratory chain in the cytoplasmic membrane, potentially providing an additional electron sink under Fe-deprived conditions [68, 69]. Furthermore, a *Synechocystis* mutant in which the *ctaD2* and *ctaE2* genes were inactivated was found to display markedly impaired Fe reduction and uptake rates as compared to wild-type cells, suggesting that ARTO is involved in the reduction of Fe(III) to Fe(II) prior to its transport through the plasma membrane via the Fe(II) transporter FeoB

[70]. Thus, the presence of the ARTO system appears to represent a major and previously unreported adaptation for *Prochlorococcus* populations thriving in low-Fe areas.

Both *Prochlorococcus* and *Synechococcus* thriving in low-Fe waters also possess eCAGs encoding the TonB-dependent siderophore uptake operon *fecDCAB-tonB-exbBD* (Pro-eCAG_015 and Syn-eCAG_013-014, Dataset 6). This gene cluster, which is found in a few picocyanobacterial genomes and was previously shown to be anti-correlated with dissolved Fe concentration [14, 15, 64], is indeed systematically present in a significant part of the *Prochlorococcus* and *Synechococcus* population in low-Fe areas (Fig. S15). However, it is also present in a small fraction of the populations thriving in the Indian Ocean, consistent with its occurrence in two *Prochlorococcus* HLII and one *Synechococcus* clade II genomes (Dataset 6). Finally, a large proportion of the *Synechococcus* populations in HNLC areas possess i) a large eCAG involved in glycine betaine synthesis and transport (Syn-eCAG_010, Fig. S15A-B; [6, 71, 72]), almost absent from low-N areas, ii) an eCAG encompassing a flavodoxin and a thioredoxin reductase (Syn-eCAG_011, Fig. S16C-D), mostly absent from low-P areas, and iii) the *nfeD-floT1-floT2* eCAG (Syn-eCAG_012, Fig. S17A-B) involved in the production of lipid rafts, potentially affecting cell shape and motility [6, 73].

<u>*eCAGs enriched in cold waters*</u>

Besides genes involved in nutrient acquisition and metabolism, several *Prochlorococcus* and *Synechococcus* eCAGs were found to be correlated with low temperature. A closer examination of *Prochlorococcus* eCAGs however, shows that their occurrence is not directly related to temperature adaptation but mainly explained by the prevalence at high latitude of either i) the HLIA ESTU (Fig. 2A, C and Fig. 4), the *red* module encompassing most of the above-mentioned eCAGs involved in P-uptake and assimilation pathways, or ii) the LLIA ESTU, present in surface waters at vertically-mixed stations, the *turquoise* module mainly gathering *Prochlorococcus* LL-specific genes, such as Pro-eCAG_017, involved in phycoerythrin-III biosynthesis (*ppeA*, *cpeFTZY*, *unk13*). As concerns *Synechococcus*, although a fairly high number of eCAGs were identified in the *tan* module associated with ESTUs IA and IVA-C (Fig. 2B, D and Fig. S4), only very few are conserved in more than two reference strains and/or have a characterized function (Dataset 6).

Among these, at least one eCAG is clearly related to adaptation to cold waters, the orange carotenoid protein (OCP) operon (*ocp-crtW-frp*; Syn-eCAG_016). Indeed, this operon is involved in a photoprotective process [74] that provides cells with the ability to deal with oxidative stress under cold temperatures [75]. Accordingly, our data shows that *Synechococcus* populations colonizing mixed waters at high latitudes or in upwelling areas all possess this eCAG (Fig. S18), highlighting the importance of this photoprotection system in *Synechococcus* populations colonizing cold and temperate areas. *Synechococcus* populations thriving in cold waters also appear to be enriched in eCAGs involved in gene regulation such as transcription factors involved in the regulation of the CA4-A form of the type IV chromatic acclimation process (*fciA-B;* Syn-eCAG_017), consistent with the predominance of *Synechococcus* CA4-A cells in temperate or cold environments [76–78](Dataset 6). Altogether, the fairly low number of eCAGs strongly associated with temperature supports the hypothesis that adaptation to cold temperature is not mediated by evolution of gene content but rather of protein sequences [5, 6, 36, 79].

Conclusions

Our analysis of *Prochlorococcus* and *Synechococcus* gene distributions at the global scale using the deeply sequenced metagenomes collected along the *Tara* Oceans expedition transect revealed that each picocyanobacterial community has a specific gene repertoire, with different sets of accessory genes being highly correlated with distinct ESTUs and physicochemical parameters. As previously suggested for *Prochlorococcus* [36], this strong correlation between taxonomy and gene content strengthens the idea that, in both genera, genome evolution mainly occurs by vertical transmission and selective gene retention, and that lateral gene transfers between ecotypes are fairly scarce. By combining information about gene synteny in 256 reference genomes with the distribution and abundance of these genes in the field, we further managed to delineate suites of adjacent genes likely involved in the same metabolic pathways that may have a crucial role in adaptation to specific niches. These analyses confirmed previous observations about the niche partitioning of individual genes and a few genomic regions involved in nutrient uptake and assimilation [14, 15, 25, 31, 33, 36, 40, 42]. Most importantly, even though our network approach likely only revealed the lower boundary of the number of eCAGs actually present in different niches, due to the incompleteness of some reference genomes, this approach highlighted that some previously detected individual genes are part of larger genomic regions and

unveiled several novel genomic regions. Although we cannot exclude that some genes enriched in a specific niche are not adaptive *per se* but either hitchhiked along with an adaptive gene [80] or occurred from passive transport of ecotype populations outside their niche [79, 81], it is reasonable to assume that many eCAGs identified in the present study could confer cells a fitness benefit in particular niches and were thus retained by natural selection, or in contrast have been counter-selected in certain environments (such as eCAGs that are absent from low-Fe environments). This study revealed the potential importance of the uptake and assimilation of organic forms of nutrients, which might either be directly used by cells e.g. for the biosynthesis of proteins or DNA, or be degraded into inorganic N and/or P forms. Consequently, many eCAGs potentially involved in the uptake and assimilation of complex compounds, such as guanidine, C≡N-containing compounds, or pyrimidine were present in both N- and P-depleted waters, and might constitute an advantage in areas of the world ocean co-limited in these nutrients [30], while they were absent from HNLC areas. Our data also suggests that adaptation to Fe-limitation relies on specific adaptation mechanisms including the reduction of Fe(III) to Fe(II) using ARTO, Fe scavenging using siderophores, as well as reduction of the Fe quota and of energy-consuming mechanisms, such as polysaccharide capsule biosynthesis. Altogether, this study provides novel insights into the genetic basis of niche partitioning in key members of the phytoplankton community. A future challenge will clearly be biochemically characterizing the function of adaptive genes in these eCAGs (Datasets 5 and 6), which are sometimes present in only a few or even a single cultured strain but which can occur in a large part or even the whole *Prochlorococcus* and/or *Synechococcus* population occupying a specific niche *in situ*.

Materials and Methods

Tara Oceans metagenomic reads from surface waters corresponding to the bacterial size-fraction [24, 82] were recruited against 256 reference genomes using MMseqs2 Release 11-e1a1c (76) and then mapped to an extended database, including 722 outgroup cyanobacterial genomes (Dataset 9; Supplementary Methods). Picocyanobacterial reads were then taxonomically assigned to either *Prochlorococcus* or *Synechococcus* and functionally assigned to a cluster of likely orthologous genes (CLOGs) as defined in the information system Cyanorak *v2.1* [19]. After normalization by gene and read length, filtration steps included the selection of i) samples containing more CLOGs

446 than the average number of genes in a *Synechococcus* or *Prochlorococcus* HL genome, ii) CLOGs
447 with a gene coverage higher than 1 in at least 2 of the selected samples and iii) non-core genes
448 [6].
449 *Tara* Oceans stations were clustered using Ward's minimum variance [83] based on Bray-
450 Curtis similarities between the relative abundance of either CLOG or picocyanobacterial ESTUs as
451 defined based on the *petB* marker gene [24]. CLOG abundance profiles were also used to perform
452 co-occurrence analyses by weighted genes correlation network analysis (WGCNA, [84, 85]) to
453 delineate modules of CLOGs that share a similar distribution pattern. The *eigengene* of each
454 module was then correlated to environmental parameters, retrieved from PANGAEA
455 (www.pangaea.de/), and to the relative abundance of *petB* ESTUs. Furthermore, the most
456 representative genes of each module were identified as those most correlated to the *eigengene*.
457 Finally, we then defined eCAGs within each module by searching adjacent genes (less than 6 genes
458 apart in 80% of the genomes possessing them) in the 256 reference genomes (Datasets 7 and 8)
459 that were used to build a network of the corresponding CLOGs (node) according to the graph
460 embedder (GEM) or the Fruchterman-Reingold layout algorithms implemented in the R package
461 igraph [86].
462 A detailed version of these methods is available in Supplementary Methods.
463

464 **Contributions**

465 HD and LG conceived and supervised the project. MR, MO, GKF, DJS, FP, LG, and PW participated
466 in the generation of genomes and/or metagenomes used in this study. UG, HD, GKF, and JL
467 performed the bioinformatics analyses. LBG, MH, JS, GL, and EC developed the Cyanorak
468 information system and FP, HD, UG, JL, MF, MO, DJS, and LG curated the genome database. UG,
469 BA, and DE performed the network and statistical analyses. HD, UG, FP, DJS, DE, and LG wrote the
470 manuscript.

471

472 **Acknowledgments**
473

This work was supported by the French “Agence Nationale de la Recherche” Programs SAMOSA (ANR-13-ADAP-0010), CINNAMON (ANR-17-CE02-0014-01), EFFICACY (ANR-19-CE02-0019), and France Génomique (ANR-10-INBS-09) as well as the European Union program Assemble+ (Horizon 2020, under grant agreement number 287589). We acknowledge Christophe Six for his help with cloning some of the *Synechococcus* strains used in this study and Francisco M. Cornejo-Castillo for helpful discussions. We also thank the support and commitment of the *Tara* Oceans coordinators and consortium, Agnès b. and E. Bourgois, the Veolia Environment Foundation, Région Bretagne, Lorient Agglomeration, World Courier, Illumina, the EDF Foundation, FRB, the Prince Albert II de Monaco Foundation, the *Tara* schooner, and its captains and crew. *Tara* Oceans would not exist without continuous support from 23 institutes (http://oceans.taraexpeditions.org).

References

1. Field CB, Behrenfeld MJ, Randerson JT, & Falkowski PG. Primary production of the biosphere: Integrating terrestrial and oceanic components. *Science* 1998; **281**: 237–240.

2. Litchman E, de Tezanos Pinto P, Edwards KF, Klausmeier CA, Kremer CT, Thomas MK. Global biogeochemical impacts of phytoplankton: a trait-based perspective. *J Ecol* 2015; **103**: 1384–1396.

3. Abonyi A, Horváth Z, Ptacnik R. Functional richness outperforms taxonomic richness in predicting ecosystem functioning in natural phytoplankton communities. *Freshwater Biol* 2018; **63**: 178–186.

4. Ye L, Chang C-W, Matsuzaki SS, Takamura N, Widdicombe CE, Hsieh C. Functional diversity promotes phytoplankton resource use efficiency. *J Ecol* 2019; **107**: 2353–2363.

5. Kettler GC, Martiny AC, Huang K, Zucker J, Coleman ML, Rodrigue S, et al. Patterns and implications of gene gain and loss in the evolution of *Prochlorococcus*. *PLoS Genet* 2007; **3**: e231.

6. Doré H, Farrant GK, Guyet U, Haguait J, Humily F, Ratin M, et al. Evolutionary mechanisms of long-term genome diversification associated with niche partitioning in marine picocyanobacteria. *Front Microbiol* 2020; **11**: 567431.

7. Nef C, Madoui M-A, Pelletier É, Bowler C. Whole-genome scanning reveals environmental selection mechanisms that shape diversity in populations of the epipelagic diatom *Chaetoceros*. *PLoS Biol* 2022; **20**: e3001893.

8. Read BA, Kegel J, Klute MJ, Kuo A, Lefebvre SC, Maumus F, et al. Pan genome of the phytoplankton *Emiliania* underpins its global distribution. *Nature* 2013; **499**: 209–213.

9. Piganeau G, Grimsley N, Moreau H. Genome diversity in the smallest marine photosynthetic eukaryotes. *Res Microbiol* 2011; **162**: 570–577.

10. Delmont TO, Eren AM. Linking pangenomes and metagenomes: the *Prochlorococcus* metapangenome. *PeerJ* 2018; **6**: e4320.

11. Tully BJ, Graham ED, Heidelberg JF. The reconstruction of 2,631 draft metagenome-assembled genomes from the global oceans. *Sci Data* 2018; **5**: 170203.

12. Massana R, López-Escardó D. Metagenome assembled genomes are for eukaryotes too. *Cell Genomics* 2022; **2**: 100130.

13. Duncan A, Barry K, Daum C, Eloe-Fadrosh E, Roux S, Schmidt K, et al. Metagenome-assembled genomes of phytoplankton microbiomes from the Arctic and Atlantic Oceans. *Microbiome* 2022; **10**: 67.

14. Garcia CA, Hagstrom GI, Larkin AA, Ustick LJ, Levin SA, Lomas MW, et al. Linking regional shifts in microbial genome adaptation with surface ocean biogeochemistry. *Phil Trans Roy Soc B Biol Sci* 2020; **375**: 20190254.

15. Ahlgren NA, Belisle BS, Lee MD. Genomic mosaicism underlies the adaptation of marine *Synechococcus* ecotypes to distinct oceanic iron niches. *Environ Microbiol* 2020; **22**: 1801–1815.

16. Garcia SL, Stevens SLR, Crary B, Martinez-Garcia M, Stepanauskas R, Woyke T, et al. Contrasting patterns of genome-level diversity across distinct co-occurring bacterial populations. *ISME J* 2018; **12**: 742–755.

17. Berube PM, Biller SJ, Hackl T, Hogle SL, Satinsky BM, Becker JW, et al. Single cell genomes of *Prochlorococcus*, *Synechococcus*, and sympatric microbes from diverse marine environments. *Sci Data* 2018; **5**: 180154.

18. Biller SJ, Berube PM, Dooley K, Williams M, Satinsky BM, Hackl T, et al. Marine microbial metagenomes sampled across space and time. *Sci Data* 2018; **5**: 180176.

19. Garczarek L, Guyet U, Doré H, Farrant GK, Hoebeke M, Brillet-Guéguen L, et al. Cyanorak v2.1: a scalable information system dedicated to the visualization and expert curation of marine and brackish picocyanobacteria genomes. *Nucl Acids Res* 2021; **49**: D667–D676.

20. Kashtan N, Roggensack SE, Rodrigue S, Thompson JW, Biller SJ, Coe A, et al. Single-cell genomics reveals hundreds of coexisting subpopulations in wild *Prochlorococcus*. *Science* 2014; **344**: 416–420.

21. Flombaum P, Gallegos JL, Gordillo R a, Rincón J, Zabala LL, Jiao N, et al. Present and future global distributions of the marine Cyanobacteria *Prochlorococcus* and *Synechococcus*. *Proc Natl Acad Sci USA* 2013; **110**: 9824–9.

22. Visintini N, Martiny AC, Flombaum P. *Prochlorococcus*, *Synechococcus*, and picoeukaryotic phytoplankton abundances in the global ocean. *Limnol Oceanogr* 2021; **6**: 207–215.

23. Paulsen ML, Doré H, Garczarek L, Seuthe L, Müller O, Sandaa R-A, et al. *Synechococcus* in the Atlantic gateway to the Arctic Ocean. *Front Mar Sci* 2016; **3**: 191.

24. Farrant GK, Doré H, Cornejo-Castillo FM, Partensky F, Ratin M, Ostrowski M, et al.

547 Delineating ecologically significant taxonomic units from global patterns of marine
548 picocyanobacteria. *Proc Natl Acad Sci USA* 2016; **113**: E3365–E3374.

549 25. Sohm JA, Ahlgren NA, Thomson ZJ, Williams C, Moffett JW, Saito MA, et al. Co-
550 occurring *Synechococcus* ecotypes occupy four major oceanic regimes defined by temperature,
551 macronutrients and iron. *ISME J* 2016; **10**: 333–345.

552 26. Ahlgren NA, Rocap G. Diversity and distribution of marine *Synechococcus*: Multiple
553 gene phylogenies for consensus classification and development of qPCR assays for sensitive
554 measurement of clades in the ocean. *Front Microbiol* 2012; **3**: 213–213.

555 27. Biller SJ, Berube PM, Lindell D, Chisholm SW. *Prochlorococcus*: The structure and
556 function of collective diversity. *Nature Rev Microbiol* 2015; **13**: 13–27.

557 28. Huang S, Wilhelm SW, Harvey HR, Taylor K, Jiao N, Chen F. Novel lineages of
558 *Prochlorococcus* and *Synechococcus* in the global oceans. *ISME J* 2012; **6**: 285–297.

559 29. Kent AG, Baer SE, Mouginot C, Huang JS, Larkin AA, Lomas MW, et al. Parallel
560 phylogeography of *Prochlorococcus* and *Synechococcus*. *ISME J* 2019; **13**: 430–441.

561 30. Ustick LJ, Larkin AA, Garcia CA, Garcia NS, Brock ML, Lee JA, et al. Metagenomic
562 analysis reveals global-scale patterns of ocean nutrient limitation. *Science* 2021; **372**: 287–291.

563 31. Martiny AC, Coleman ML, Chisholm SW. Phosphate acquisition genes in
564 *Prochlorococcus* ecotypes: Evidence for genome-wide adaptation. *Proc Natl Acad Sci USA* 2006;
565 **103**: 12552–12557.

566 32. Martiny AC, Huang Y, Li W. Occurrence of phosphate acquisition genes in
567 *Prochlorococcus* cells from different ocean regions. *Environ Microbiol* 2009; **11**: 1340–1347.

568 33. Kashtan N, Roggensack SE, Berta-Thompson JW, Grinberg M, Stepanauskas R,
569 Chisholm SW. Fundamental differences in diversity and genomic population structure between
570 Atlantic and Pacific *Prochlorococcus*. *ISME J* 2017; **11**: 1997–2011.

571 34. Zheng Y, Roberts RJ, Kasif S. Genomic functional annotation using co-evolution profiles
572 of gene clusters. *Genome Biol* 2002; **3**: research0060.1.

573 35. Overbeek R, Fonstein M, D'Souza M, Pusch GD, Maltsev N. The use of gene clusters to
574 infer functional coupling. *Proc Natl Acad Sci USA* 1999; **96**: 2896–2901.

575 36. Kent AG, Dupont CL, Yooseph S, Martiny AC. Global biogeography of
576 *Prochlorococcus* genome diversity in the surface ocean. *ISME J* 2016; **10**: 1856–1865.

577 37. Song Q, Gordon AL, Visbeck M. Spreading of the Indonesian throughflow in the Indian
578 Ocean. *J Phys Oceanogr* 2004; **34**: 772–792.

579 38. West NJ, Lebaron P, Strutton PG, Suzuki MT. A novel clade of *Prochlorococcus* found
580 in high nutrient low chlorophyll waters in the South and Equatorial Pacific Ocean. *ISME J* 2011;
581 **5**: 933–944.

582 39. Rusch DB, Martiny AC, Dupont CL, Halpern AL, Venter JC. Characterization of
583 *Prochlorococcus* clades from iron-depleted oceanic regions. *Proc Natl Acad Sci USA* 2010; **107**:

16184–16189.

40. Martiny AC, Kathuria S, Berube PM. Widespread metabolic potential for nitrite and nitrate assimilation among *Prochlorococcus* ecotypes. *Proc Natl Acad Sci USA* 2009; **106**: 10787–10792.

41. Berube PM, Rasmussen A, Braakman R, Stepanauskas R, Chisholm SW. Emergence of trait variability through the lens of nitrogen assimilation in *Prochlorococcus*. *eLife* 2019; **8**: e41043–e41043.

42. Berube PM, Biller SJ, Kent AG, Berta-Thompson JW, Roggensack SE, Roache-Johnson KH, et al. Physiology and evolution of nitrate acquisition in *Prochlorococcus*. *ISME J* 2015.

43. Burnat M, Li B, Kim SH, Michael AJ, Flores E. Homospermidine biosynthesis in the cyanobacterium *Anabaena* requires a deoxyhypusine synthase homologue and is essential for normal diazotrophic growth. *Mol Microbiol* 2018; **109**: 763–780.

44. Wang B, Xu Y, Wang X, Yuan JS, Johnson CH, Young JD, et al. A guanidine-degrading enzyme controls genomic stability of ethylene-producing cyanobacteria. *Nat Commun* 2021; **12**: 5150.

45. Nelson JW, Atilho RM, Sherlock ME, Stockbridge RB, Breaker RR. Metabolism of free guanidine in Bacteria is regulated by a widespread riboswitch class. *Mol Cell* 2017; **65**: 220–230.

46. Novichkov PS, Kazakov AE, Ravcheev DA, Leyn SA, Kovaleva GY, Sutormin RA, et al. RegPrecise 3.0 – A resource for genome-scale exploration of transcriptional regulation in bacteria. *BMC Genomics* 2013; **14**: 745.

47. Kamennaya NA, Post AF. Characterization of cyanate metabolism in marine *Synechococcus* and *Prochlorococcus* spp. *Appl Environ Microbiol* 2011; **77**: 291–301.

48. Kamennaya NA, Post AF. Distribution and expression of the cyanate acquisition potential among cyanobacterial populations in oligotrophic marine waters. *Limnol Oceanogr* 2013; **58**: 1959–1971.

49. Jones LB, Ghosh P, Lee J-H, Chou C-N, Kunz DAY 2018. Linkage of the Nit1C gene cluster to bacterial cyanide assimilation as a nitrogen source. *Microbiol* 2018; **164**: 956–968.

50. Pablo F, Stauber JL, Buckney RT. Toxicity of cyanide and cyanide complexes to the marine diatom *Nitzschia closterium*. *Water Res* 1997; **31**: 2435–2442.

51. Saunders JK, Rocap G. Genomic potential for arsenic efflux and methylation varies among global *Prochlorococcus* populations. *ISME J* 2016; **10**: 197–209.

52. Riedel GF. Influence of salinity and sulfate on the toxicity of chromium(vi) to the estuarine diatom *Thalassiosira Pseudonana*. *J Phycol* 1984; **20**: 496–500.

53. Pernil R, Picossi S, Mariscal V, Herrero A, Flores E. ABC-type amino acid uptake transporters Bgt and N-II of *Anabaena* sp. strain PCC 7120 share an ATPase subunit and are expressed in vegetative cells and heterocysts. *Mol Microbiol* 2008; **67**: 1067–1080.

54. Coleman ML, Sullivan MB, Martiny AC, Steglich C, Barry K, Delong EF, et al.

621 Genomic islands and the ecology and evolution of *Prochlorococcus*. *Science* 2006; **311**: 1768–
622 1770.

623 55. Moore CM, Mills MM, Arrigo KR, Berman-Frank I, Bopp L, Boyd PW, et al. Processes
624 and patterns of oceanic nutrient limitation. *Nature Geosci* 2013; **6**: 701–710.

625 56. Tetu SG, Brahamsha B, Johnson DA, Tai V, Phillippy K, Palenik B, et al. Microarray
626 analysis of phosphate regulation in the marine cyanobacterium *Synechococcus* sp. WH8102.
627 *ISME J* 2009; **3**: 835–849.

628 57. Clark LL, Ingall ED, Benner R. Marine phosphorus is selectively remineralized. *Nature*
629 1998; **393**: 426–426.

630 58. Feingersch R, Philosof A, Mejuch T, Glaser F, Alalouf O, Shoham Y, et al. Potential for
631 phosphite and phosphonate utilization by *Prochlorococcus*. *ISME J* 2012; **6**: 827–834.

632 59. Martinez A, Tyson GW, Delong EF. Widespread known and novel phosphonate
633 utilization pathways in marine bacteria revealed by functional screening and metagenomic
634 analyses. *Environ Microbiol* 2010; **12**: 222–238.

635 60. Sosa OA, Casey JR, Karl DM. Methylphosphonate oxidation in *Prochlorococcus* strain
636 MIT9301 supports phosphate acquisition, formate excretion, and carbon assimilation into purines.
637 *Appl Environ Microbiol* 2019; **85**: e00289-19.

638 61. Martínez A, Osburne MS, Sharma AK, DeLong EF, Chisholm SW. Phosphite utilization
639 by the marine picocyanobacterium *Prochlorococcus* MIT9301. *Environ Microbiol* 2012; **14**:
640 1363–1377.

641 62. McSorley FR, Wyatt PB, Martinez A, DeLong EF, Hove-Jensen B, Zechel DL. PhnY and
642 PhnZ comprise a new oxidative pathway for enzymatic cleavage of a carbon–phosphorus bond. *J*
643 *Am Chem Soc* 2012; **134**: 8364–8367.

644 63. Acker M, Hogle SL, Berube PM, Hackl T, Coe A, Stepanauskas R, et al. Phosphonate
645 production by marine microbes: Exploring new sources and potential function. *Proc Natl Acad*
646 *Sci USA* 2022; **119**: e2113386119.

647 64. Malmstrom RR, Rodrigue S, Huang KH, Kelly L, Kern SE, Thompson A, et al. Ecology
648 of uncultured *Prochlorococcus* clades revealed through single-cell genomics and biogeographic
649 analysis. *ISME J* 2013; **7**: 184–198.

650 65. Cooley JW, Vermaas WFJ. Succinate dehydrogenase and other respiratory pathways in
651 thylakoid membranes of *Synechocystis* sp. strain PCC 6803: capacity comparisons and
652 physiological function. *J Bacteriol* 2001; **183**: 4251–4258.

653 66. Whitfield C. Biosynthesis and assembly of capsular polysaccharides in *Escherichia coli*.
654 *Annu Rev Biochem* 2006; **75**: 39–68.

655 67. Buffet A, Rocha EPC, Rendueles O. Nutrient conditions are primary drivers of bacterial
656 capsule maintenance in *Klebsiella*. *Proc Roy Soc B Biol Sci* 2021; **288**: 20202876.

657 68. Lea-Smith DJ, Ross N, Zori M, Bendall DS, Dennis JS, Scott SA, et al. Thylakoid
658 terminal oxidases are essential for the cyanobacterium *Synechocystis* sp. PCC 6803 to survive

659 rapidly changing light intensities. *Plant Physiol* 2013; **162**: 484–495.

660 69. Lea-Smith DJ, Bombelli P, Vasudevan R, Howe CJ. Photosynthetic, respiratory and
661 extracellular electron transport pathways in cyanobacteria. *Biochim Biophys Acta Bioenerget*
662 2016; **1857**: 247–255.

663 70. Kranzler C, Lis H, Finkel OM, Schmetterer G, Shaked Y, Keren N. Coordinated
664 transporter activity shapes high-affinity iron acquisition in cyanobacteria. *ISME J* 2014; **8**: 409–
665 417.

666 71. Scanlan DJ, Ostrowski M, Mazard S, Dufresne A, Garczarek L, Hess WR, et al.
667 Ecological genomics of marine picocyanobacteria. *Microbiol Mol Biol Rev* 2009; **73**: 249–299.

668 72. Ford BA, Ranjit P, Mabbutt BC, Paulsen IT, Shah BS. ProX from marine *Synechococcus*
669 spp. show a sole preference for glycine-betaine with differential affinity between ecotypes.
670 *Environ Microbiol* 2022**; 24:** 6071– 6085.

671 73. Dempwolff F, Wischhusen HM, Specht M, Graumann PL. The deletion of bacterial
672 dynamin and flotillin genes results in pleiotrophic effects on cell division, cell growth and in cell
673 shape maintenance. *BMC Microbiol* 2012; **12**: 298.

674 74. Boulay C, Wilson A, D'Haene S, Kirilovsky D. Identification of a protein required for
675 recovery of full antenna capacity in OCP-related photoprotective mechanism in cyanobacteria.
676 *Proc Natl Acad Sci USA* 2010; **107**: 11620–11625.

677 75. Six C, Ratin M, Marie D, Corre E. Marine *Synechococcus* picocyanobacteria: Light
678 utilization across latitudes. *Proc Natl Acad Sci USA* 2021; **118**.

679 76. Xia X, Partensky F, Garczarek L, Suzuki K, Guo C, Yan Cheung S, et al.
680 Phylogeography and pigment type diversity of *Synechococcus* cyanobacteria in surface waters of
681 the northwestern Pacific Ocean. *Environ Microbiol* 2017; **19**: 142–158.

682 77. Grébert T, Doré H, Partensky F, Farrant GK, Boss ES, Picheral M, et al. Light color
683 acclimation is a key process in the global ocean distribution of *Synechococcus* cyanobacteria.
684 *Proc Natl Acad Sci USA* 2018; **115**: E2010–E2019.

685 78. Sanfilippo JE, Nguyen AA, Karty JA, Shukla A, Schluchter WM, Garczarek L, et al.
686 Self-regulating genomic island encoding tandem regulators confers chromatic acclimation to
687 marine *Synechococcus*. *Proc Natl Acad Sci USA* 2016; **113**: 6077–6082.

688 79. Larkin AA, Martiny AC. Microdiversity shapes the traits, niche space, and biogeography
689 of microbial taxa: The ecological function of microdiversity. *Environ Microbiol Rep* 2017; **9**: 55–
690 70.

691 80. Barton NH. Genetic hitchhiking. *Philosophical Transactions of the Royal Society of*
692 *London Series B: Biological Sciences* 2000; **355**: 1553–1562.

693 81. Wiedenbeck J, Cohan FM. Origins of bacterial diversity through horizontal genetic
694 transfer and adaptation to new ecological niches. *FEMS Microbiol Rev* 2011; **35**: 957–976.

695 82. Sunagawa S, Coelho LP, Chaffron S, Kultima JR, Labadie K, Salazar G, et al. Structure
696 and function of the global ocean microbiome. *Science* 2015; **348**: 1261359–1261359.

83. Szmrecsanyi B. Grammatical variation in British English dialects: A study in corpus-based dialectometry. 2012. Cambridge University Press, Cambridge.

84. Zhang B, Horvath S. A general framework for weighted gene co-expression network analysis. *Stat Appl Genet Mol Biol* 2005; **4**: Article17.

85. Langfelder P, Horvath S. WGCNA: an R package for weighted correlation network analysis. *BMC Bioinfo* 2008; **9**: 559.

86. Csardi G, Nepusz T. The igraph software package for complex network research. *InterJournal, Complex Systems*. 2006. 1695

Figure Legends

Figure 1. Comparison of clustering based on relative abundance profiles of ecologically significant taxonomic units (ESTUs) and of flexible genes for both picocyanobacteria. A. *Prochlorococcus*. B. *Synechococcus*. Leaves of the trees correspond to stations along the *Tara* Oceans transect that are colored according to the code shown at the bottom of the trees, which corresponds to ESTU assemblages as determined previously [24] by clustering stations exhibiting similar ESTU relative abundance profiles shown here on the right of each tree (for global distribution maps of ESTU assemblages, see Fig. 3B and 4B in [24]). ESTUs were colored according to the palette below each panel. Dotted lines in dendrograms indicate discrepancies between tree topologies. Accessory genes correspond to all genes except those defined as large-core genes in a previous study [6]. Of note, due to a slightly different clustering method (cf. materials and methods), assemblage 7 (dark grey stations in 1B), which was discriminated from assemblage 6 in the Farrant et al. (2016) now clusters with this assemblage. Abbreviations: IO, Indian Ocean; MS, Mediterranean Sea; NAO, North Atlantic Ocean; NPO, North Pacific Ocean; RS, Red Sea; SAO, South Atlantic Ocean; SO, Southern Ocean.

Figure 2. Correlation of picocyanobacterial module eigengenes to physico-chemical parameters and ESTU abundance. A, B. Correlation of module eigengenes to physico-chemical parameters for *Prochlorococcus* (A) and *Synechococcus* (B). C, D. Correlation of module eigengenes to relative abundance profiles of ESTUs *sensu* [4]. Pearson (A, B) and Spearman (C, D) correlation coefficients (*r* and rho, respectively) are indicated by the color scale. Each module is identified by a specific color and the number between brackets specifies the number of genes in each module. The *eigengene* is representative of the relative abundance of genes of a given module at each *Tara* Oceans station. Non-significant correlations (Student asymptotic *p* value > 0.01) are marked by a cross. Φsat: index of iron limitation derived from satellite data. PAR30: satellite-derived photosynthetically available radiation at the surface, averaged on 30 days. DCM: depth of the deep chlorophyll maximum.

Figure 3. Violin plots highlighting the most representative genes of each *Prochlorococcus* module. For each module, each gene is represented as a dot positioned according to its

correlation with the eigengene for each module, the most representative genes being localized on top of each violin plot. Genes mentioned in the text and/or in Dataset 6 have been colored according to the color of the corresponding module, indicated by a colored bar above each module. The text above violin plots indicates the most significant environmental parameter(s) and/or ESTU(s) for each module, as derived from Fig. 2.

Figure 4. Delineation of *Prochlorococcus* eCAGs, defined as a set of genes that are both adjacent in reference genomes and share a similar *in situ* distribution. Nodes correspond to individual genes with their gene name (or significant numbers of the CK number, e.g. 1234 for CK_00001234) and are colored according to their WGCNA module. A link between two nodes indicates that these two genes are less than five genes apart in at least one genome. The bottom insert shows the most significant environmental parameter(s) and/or ESTU(s) for each module, as derived from Fig. 2.

Figure 5. Global distribution map of the eCAG involved in nitrile or cyanide transport and assimilation. (*A*) *Prochlorococcus* (Pro-eCAG_006) and (*B*) *Synechococcus* Syn-eCAG_002. (*C*) The genomic region in *Prochlorococcus marinus* MIT9301. The size of the circle is proportional to relative abundance of each genus as estimated based on the single-copy core gene *petB* and this gene was also used to estimate the relative abundance of other genes in the population. Black dots represent *Tara* Oceans stations for which *Prochlorococcus* or *Synechococcus* read abundance was too low to reach the threshold limit.

Figure 6. Global distribution map of eCAGs putatively involved in phosphonate and phosphite transport and assimilation. *Prochlorococcus* (*A*) Pro-eCAG_012 putatively involved in phosphonate transport, (*B*) Pro-eCAG_013, involved in phosphonate/phosphite uptake and assimilation and phosphonate C-P bond cleavage, (*C*) The genomic region encompassing both *phnC2-D2-E2-E3* and *ptxABDC-phnYZ* specific to *P. marinus* RS01. The size of the circle is proportional to relative abundance of *Prochlorococcus* as estimated based on the single-copy core gene *petB* and this gene was also used to estimate the relative abundance of other genes in the

767 population. Black dots represent *Tara* Oceans stations for which *Prochlorococcus* read abundance
768 was too low to reach the threshold limit.
769
770 **Figure 7. Global distribution map of the *Prochlorococcus* eCAGs involved in the biosynthesis of**
771 **an alternative respiratory terminal oxidase (ARTO).** (*A*) *Prochlorococcus* Pro-eCAG_016, (*B*)
772 *Synechococcus* Syn-eCAG_015. The size of the circle is proportional to relative abundance of each
773 genus as estimated based on the single-copy core gene *petB* and this gene was also used to
774 estimate the relative abundance of other genes in the population. Black dots represent *Tara*
775 Oceans stations for which *Prochlorococcus* or *Synechococcus* read abundance was too low to
776 reach the threshold limit.

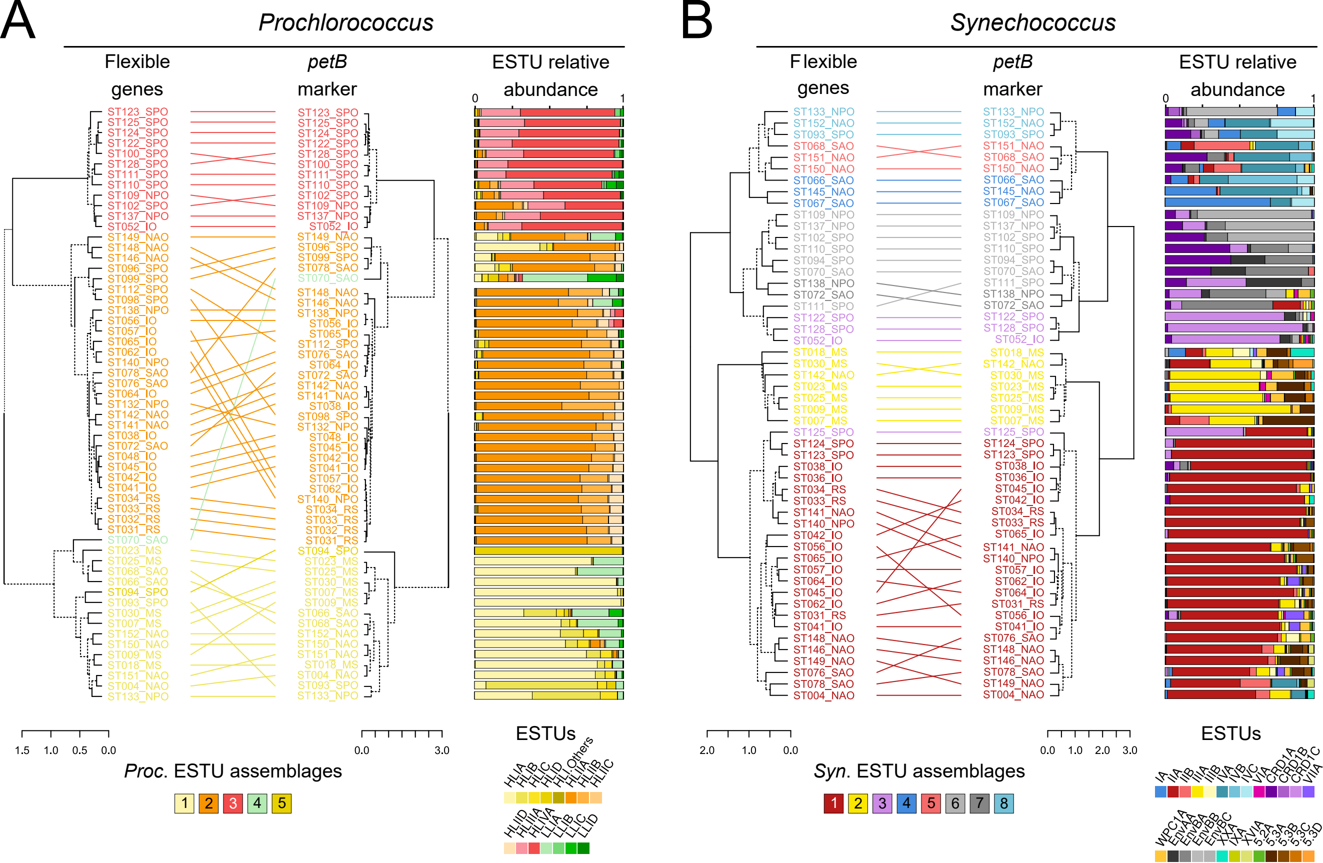
A
Prochlorococcus
Flexible genes
petB marker
ESTU relative abundance
0
1
1.5
1.0
0.5
0.0
0.0
3.0
Proc. ESTU assemblages
1
2
3
4
5
ESTUs
HLIA
HLIB
HLIC
HLID
HLI Others
HLIIA
HLIIB
HLIIC
HLIID
HLIIIA
HLIVA
LLIA
LLIB
LLIC
LLID
B
Synechococcus
Flexible genes
petB marker
ESTU relative abundance
0
1
2.0
1.0
0.0
0.0
1.0
2.0
3.0
Syn. ESTU assemblages
1
2
3
4
5
6
7
8
ESTUs
IA
IIA
IIB
IIIA
IIIB
IVA
IVB
IVC
VIA
CRD1A
CRD1B
CRD1C
VIIA
WPC1A
EnvAA
EnvBA
EnvBB
EnvBC
XXA
IXA
XVIA
5.2A
5.3A
5.3B
5.3C
5.3D

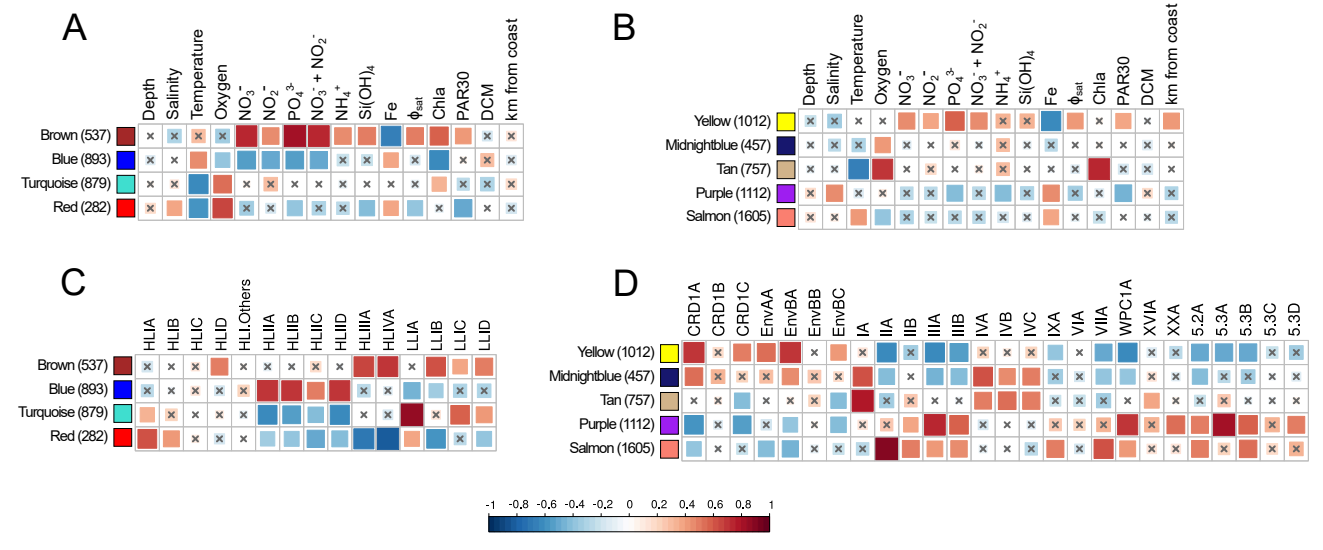
A
Depth
Salinity
Temperature
Oxygen
NO_3^-
NO_2^-
PO_4^{3-}
$NO_3^- + NO_2^-$
NH_4^+
$Si(OH)_4$
Fe
ϕ_{sat}
Chla
PAR30
DCM
km from coast
Brown (537)
Blue (893)
Turquoise (879)
Red (282)
B
Depth
Salinity
Temperature
Oxygen
NO_3^-
NO_2^-
PO_4^{3-}
$NO_3^- + NO_2^-$
NH_4^+
$Si(OH)_4$
Fe
ϕ_{sat}
Chla
PAR30
DCM
km from coast
Yellow (1012)
Midnightblue (457)
Tan (757)
Purple (1112)
Salmon (1605)
C
HLIA
HLIB
HLIC
HLID
HLI.Others
HLIIA
HLIIB
HLIIC
HLIID
HLIIIA
HLIVA
LLIA
LLIB
LLIC
LLID
Brown (537)
Blue (893)
Turquoise (879)
Red (282)
D
CRD1A
CRD1B
CRD1C
EnvAA
EnvBA
EnvBB
EnvBC
IA
IIA
IIB
IIIA
IIIB
IVA
IVB
IVC
IXA
VIA
VIIA
WPC1A
XVIA
XXA
5.2A
5.3A
5.3B
5.3C
5.3D
Yellow (1012)
Midnightblue (457)
Tan (757)
Purple (1112)
Salmon (1605)
-1
-0.8
-0.6
-0.4
-0.2
0
0.2
0.4
0.6
0.8
1

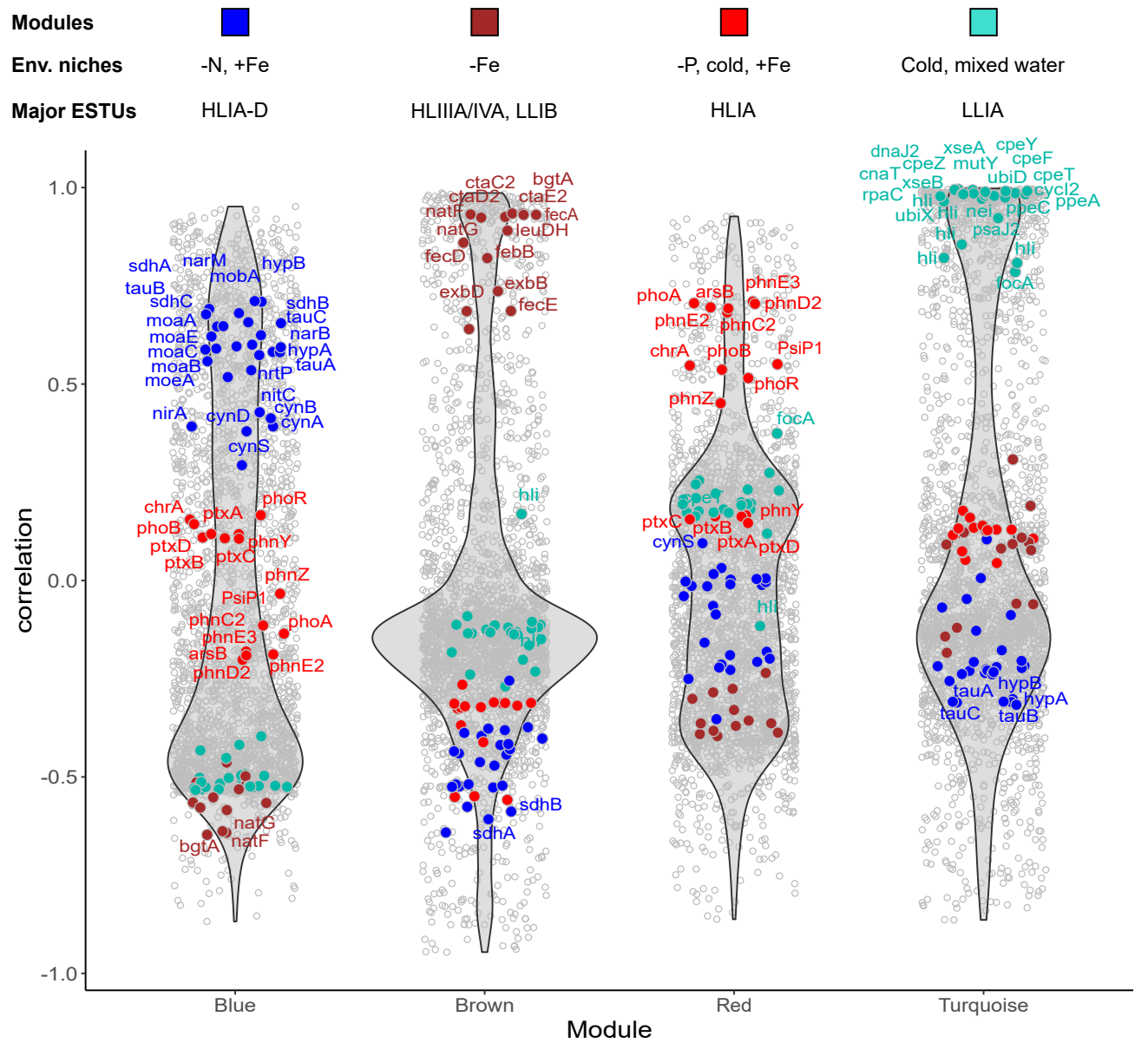
Modules
Env. niches
-N, +Fe
-Fe
-P, cold, +Fe
Cold, mixed water
Major ESTUs
HLIA-D
HLIIIA/IVA, LLIB
HLIA
LLIA
correlation
1.0
0.5
0.0
-0.5
-1.0
Blue
Brown
Red
Turquoise
Module
sdhA narM hypB
tauB mobA
sdhC sdhB
moaA tauC
moaE narB
moaC hypA
moaB tauA
moeA hrtP
nitC
nirA cynD cynB
cynA
cynS
chrA ptxA phoR
phoB phnY
ptxD ptxC
ptxB phnZ
PsiP1
phnC2 phoA
phnE3
arsB phnE2
phnD2
natG
bgtA natF
ctaC2 bgtA
ctaD2 ctaE2
natR fecA
natG leuDH
fecD febB
exbD exbB
fecE
hli
sdhB
sdhA
phoA arsB phnE3
phnE2 phnD2
phnC2
chrA phoB PsiP1
phoR
phnZ focA
ptxC phnY
ptxB
cynS ptxA ptxD
hli
dnaJ2 xseA cpeY
cpeZ mutY cpeF
cnaT xseB ubiD cpeT
rpaC hli cycl2
ubiX hli nei ppeC ppeA
hli psaJ2
hli hli
focA
tauA hypB
hypA
tauC tauB

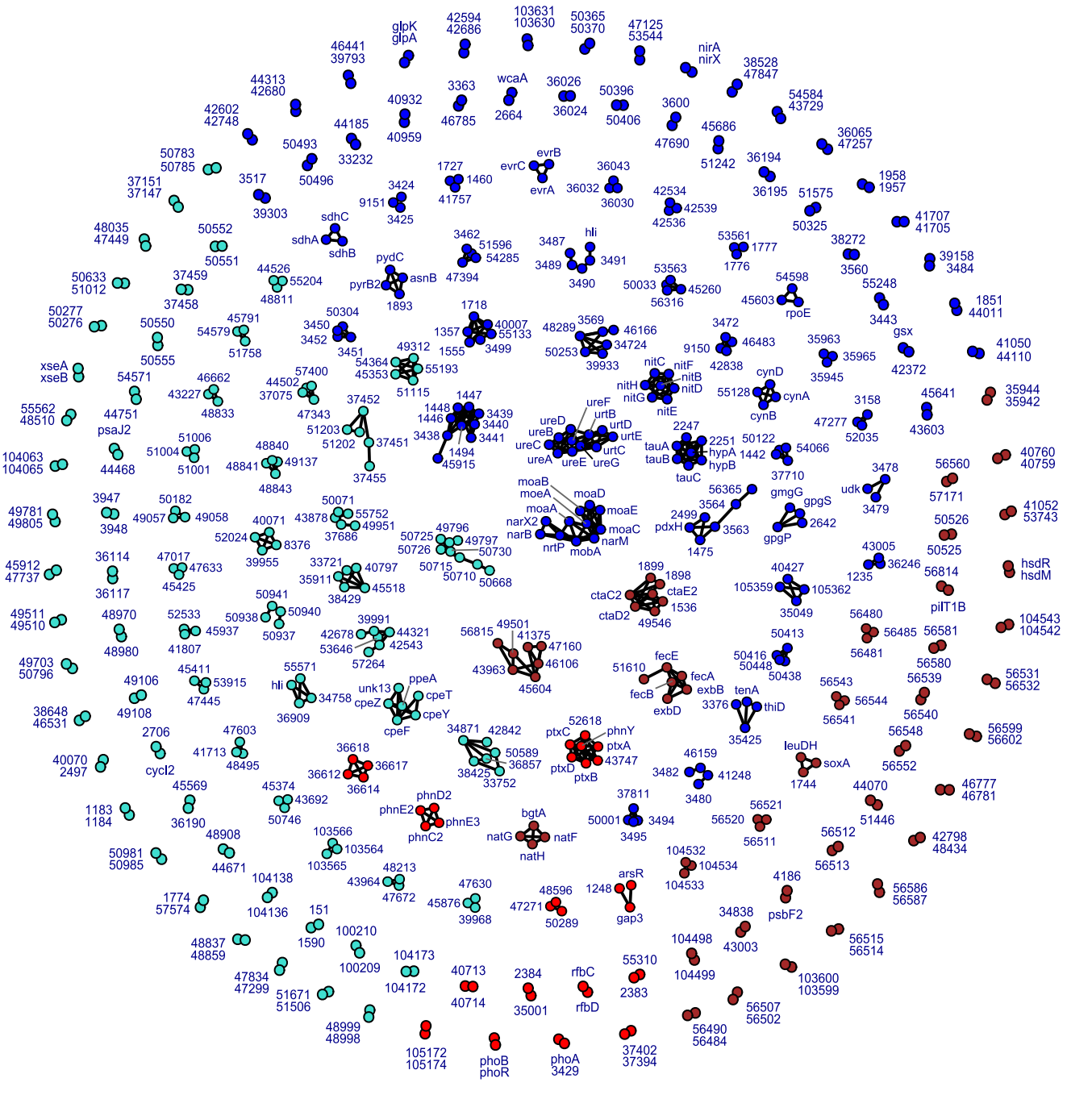
Modules
Env. niches
-N, +Fe
-Fe
-P, cold, +Fe
Cold, mixed water
Major ESTUs
HLIA-D
HLIIIA/IVA, LLIB
HLIA
LLIA

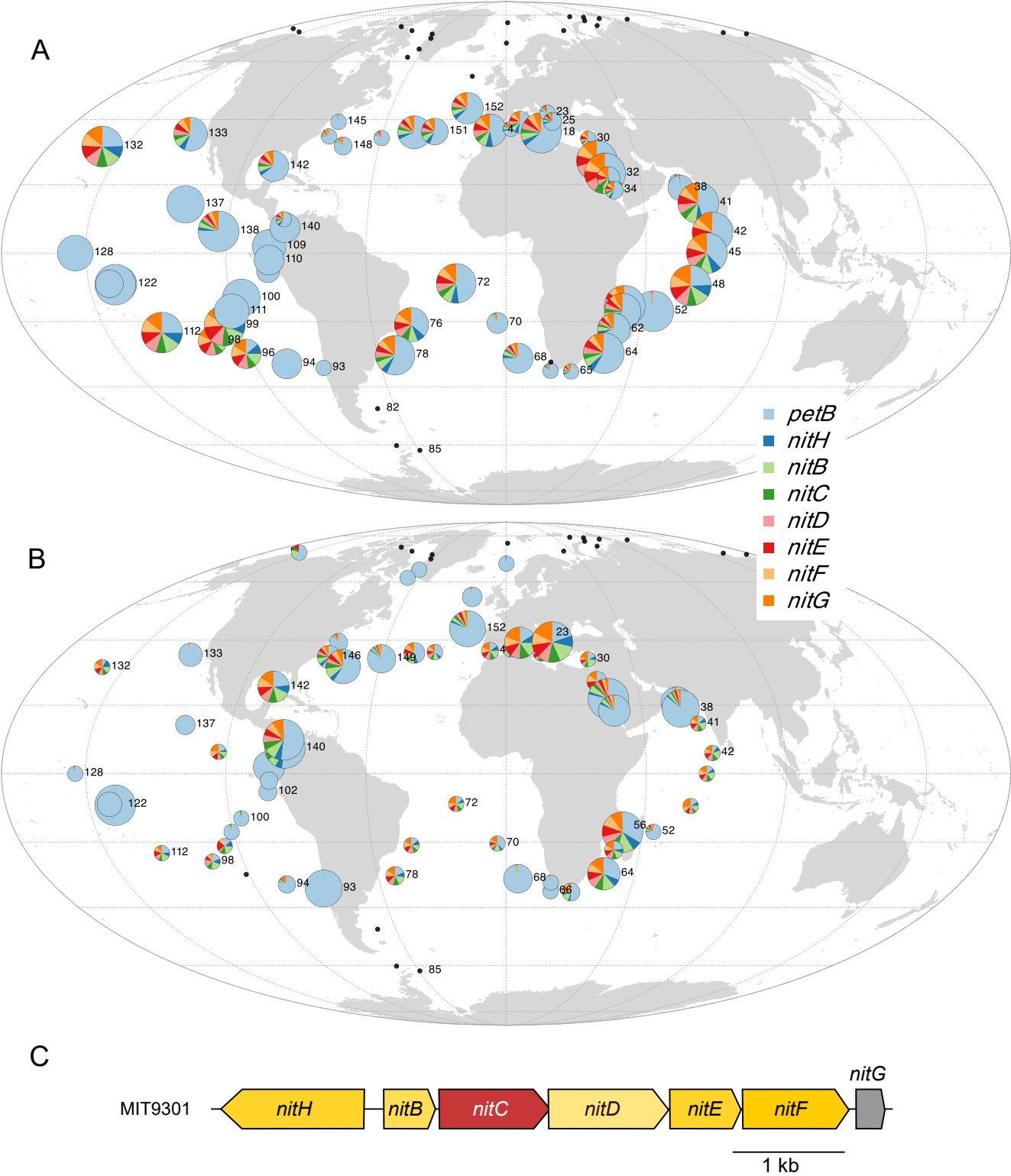
A
B
C
petB
nitH
nitB
nitC
nitD
nitE
nitF
nitG
MIT9301
1 kb

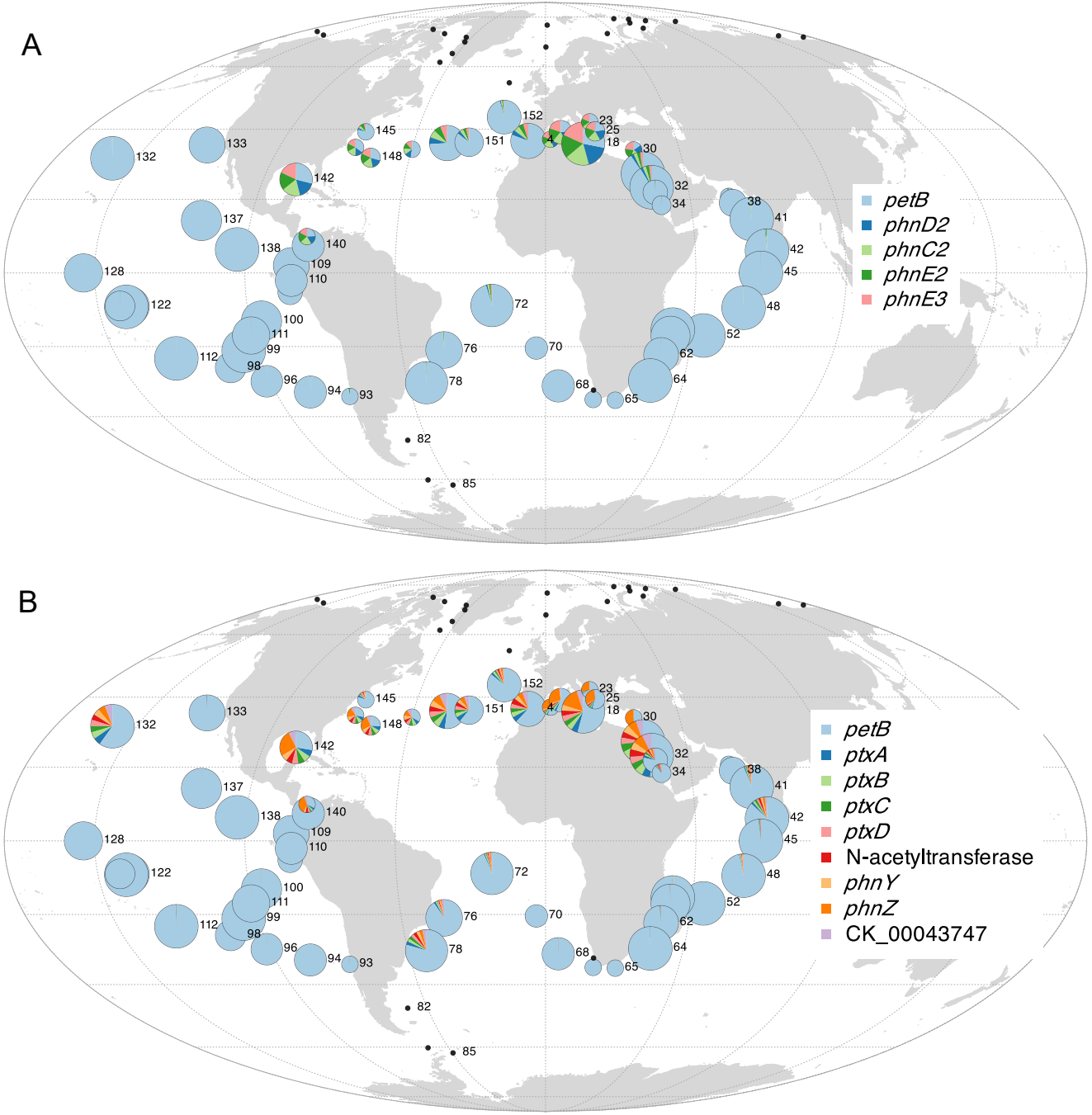
A
petB
phnD2
phnC2
phnE2
phnE3
B
petB
ptxA
ptxB
ptxC
ptxD
N-acetyltransferase
phnY
phnZ
CK_00043747
C
N-acetyltransferase
(CK_00052618)
RS01
phnD2
phnC2
phnE2
phnE3
ptxA
ptxB
ptxC
ptxD
phnY
phnZ
1 kb

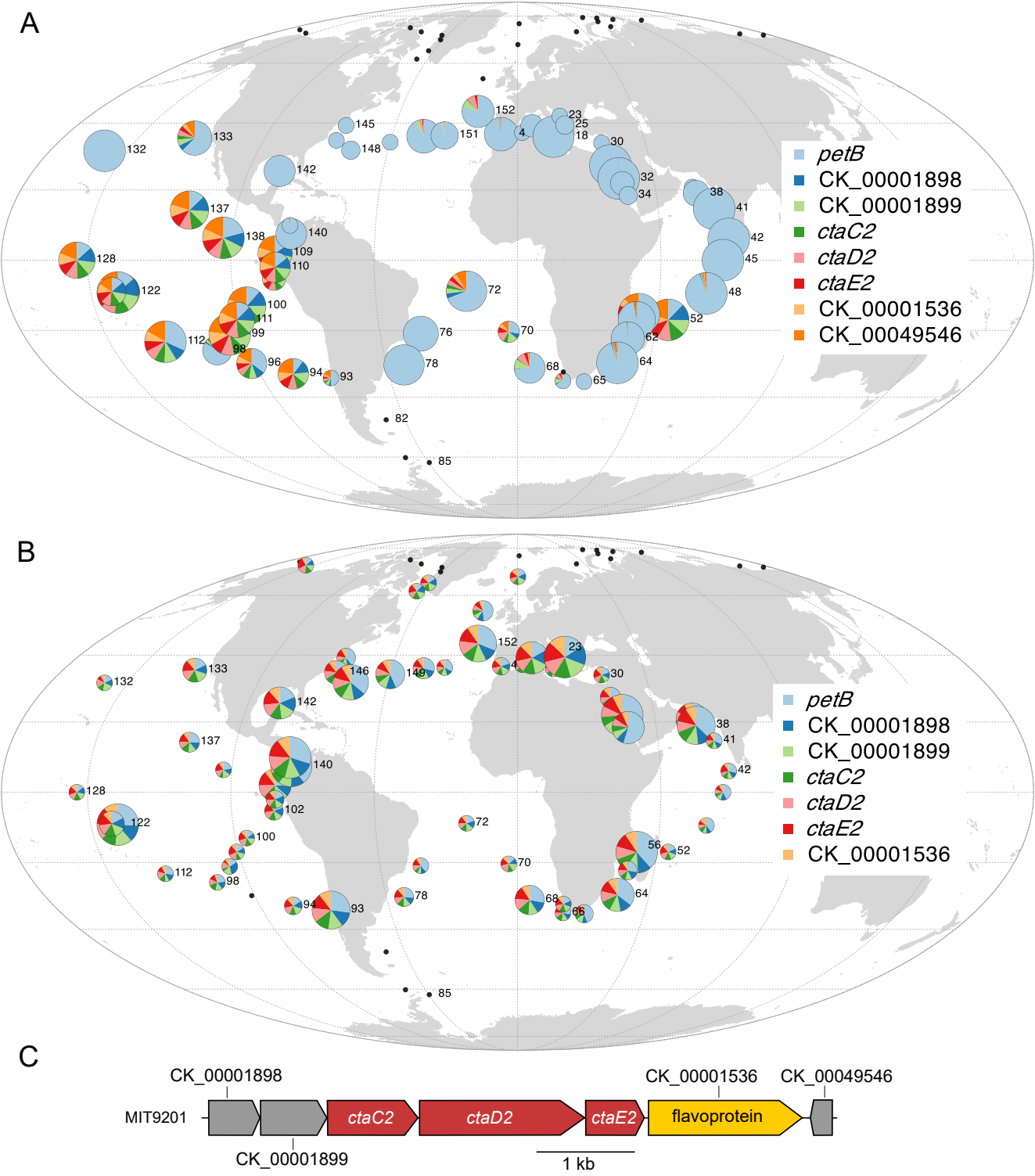
A
B
C
petB
CK_00001898
CK_00001899
ctaC2
ctaD2
ctaE2
CK_00001536
CK_00049546
MIT9201
flavoprotein
1 kb